



*remote sensing*



Technical Note

---

# Ecosystem Integrity Remote Sensing—Modelling and Service Tool—ESIS/Imalys

---

Peter Selsam, Jan Bumberger, Thilo Wellmann, Marion Pause, Ronny Gey, Erik Borg and Angela Lausch



<https://doi.org/10.3390/rs16071139>



Technical Note

# Ecosystem Integrity Remote Sensing—Modelling and Service Tool—ESIS/Imalys

Peter Selsam <sup>1,2</sup>, Jan Bumberger <sup>1,2,3</sup>, Thilo Wellmann <sup>4</sup>, Marion Pause <sup>5</sup>, Ronny Gey <sup>1,2</sup>, Erik Borg <sup>6,7</sup> and Angela Lausch <sup>5,8,9,\*</sup>

- <sup>1</sup> Department of Monitoring and Exploration Technologies, Helmholtz Centre for Environmental Research—UFZ, Permoserstr. 15, D-04318 Leipzig, Germany; peter.selsam@ufz.de (P.S.); jan.bumberger@ufz.de (J.B.); ronny.hey@ufz.de (R.G.)
- <sup>2</sup> Research Data Management—RDM, Helmholtz Centre for Environmental Research GmbH—UFZ, Permoserstraße 15, D-04318 Leipzig, Germany
- <sup>3</sup> German Centre for Integrative Biodiversity Research (iDiv) Halle-Jena-Leipzig, Puschestraße 4, D-04103 Leipzig, Germany
- <sup>4</sup> Landscape Ecology Lab, Geography Department, Humboldt-Universität zu Berlin, Unter den Linden 6, D-10099 Berlin, Germany; thilo.wellmann@hu-berlin.de
- <sup>5</sup> Department of Architecture, Facility Management and Geoinformation, Institute for Geoinformation and Surveying, Bauhausstraße 8, D-06846 Dessau, Germany; marion.pause@hs-anhalt.de
- <sup>6</sup> Deutsches Fernerkundungsdatenzentrum-DFD, Deutsches Zentrum für Luft- und Raumfahrt-DLR, Kalkhorstweg 53, D-17235 Neustrelitz, Germany; erik.borg@dlr.de
- <sup>7</sup> Geodäsie und Geoinformatik, Fachhochschule Neubrandenburg, Brodaer Straße 2, D-17033 Neubrandenburg, Germany
- <sup>8</sup> Department of Computational Landscape Ecology, Helmholtz Centre for Environmental Research—UFZ, Permoserstr. 15, D-04318 Leipzig, Germany
- <sup>9</sup> Department of Physical Geography and Geoecology, Martin Luther University Halle-Wittenberg, Von-Seckendorff-Platz 4, D-06120 Halle, Germany
- \* Correspondence: angela.lausch@ufz.de; Tel.: +49-341-235-1961; Fax: +49-341-235-1939

**Abstract:** One of the greatest challenges of our time is monitoring the rapid environmental changes taking place worldwide at both local and global scales. This requires easy-to-use and ready-to-implement tools and services to monitor and quantify aspects of bio- and geodiversity change and the impact of land use intensification using freely available and global remotely sensed data, and to derive remotely sensed indicators. Currently, there are no services for quantifying both raster- and vector-based indicators in a “compact tool”. Therefore, the main innovation of ESIS/Imalys is having a remote sensing (RS) tool that allows for RS data processing, data management, and continuous and discrete quantification and derivation of RS indicators in one tool. With the ESIS/Imalys project (Ecosystem Integrity Remote Sensing—Modelling and Service Tool), we try to present environmental indicators on a clearly defined and reproducible basis. The Imalys software library generates the RS indicators and remote sensing products defined for ESIS. This paper provides an overview of the functionality of the Imalys software library. An overview of the technical background of the implementation of the Imalys library, data formats and the user interfaces is given. Examples of RS-based indicators derived using the Imalys tool at pixel level and at zone level (vector level) are presented. Furthermore, the advantages and disadvantages of the Imalys tool are discussed in detail in order to better assess the value of Imalys for users and developers. The applicability of the indicators will be demonstrated through three ecological applications, namely: (1) monitoring landscape diversity, (2) monitoring landscape structure and landscape fragmentation, and (3) monitoring land use intensity and its impact on ecosystem functions. Despite the integration of large amounts of data, Imalys can run on any PC, as the processing and derivation of indicators has been greatly optimised. The Imalys source code is freely available and is hosted and maintained under an open source license. Complete documentation of all methods, functions and derived indicators can be found in the freely available Imalys manual. The user-friendliness of Imalys, despite the integration of a large amount of RS data, makes it another important tool for ecological research, modelling and application for the monitoring and derivation of ecosystem indicators from local to global scale.



**Citation:** Selsam, P.; Bumberger, J.; Wellmann, T.; Pause, M.; Gey, R.; Borg, E.; Lausch, A. Ecosystem Integrity Remote Sensing—Modelling and Service Tool—ESIS/Imalys. *Remote Sens.* **2024**, *16*, 1139. <https://doi.org/10.3390/rs16071139>

Academic Editor: Qinghua Guo

Received: 8 February 2024

Revised: 15 March 2024

Accepted: 20 March 2024

Published: 25 March 2024



**Copyright:** © 2024 by the authors. Licensee MDPI, Basel, Switzerland. This article is an open access article distributed under the terms and conditions of the Creative Commons Attribution (CC BY) license (<https://creativecommons.org/licenses/by/4.0/>).

**Keywords:** ecosystem integrity; traits; spectral traits; remote sensing; earth observation; tool; service; indicators; classification; segmentation; time series; processing platform; big data; Imalys; ESIS

## 1. Introduction

Climate change, land use intensity, biological invasions and loss of bio- and geodiversity are causing rapid environmental changes around the world, ranging from having local- to global-scale impact [1]. There is therefore an urgent need for operational monitoring and surveillance tools that take into account aspects of changing biodiversity [2], geodiversity [3–5] and, in particular, to monitor status and effects of land use intensification [6]. Landscapes and their processes and changes are complex, and the influence of drivers is multidimensional. Therefore, complex multidimensional approaches such as the monitoring concept of ecosystem integrity are needed to better understand the causes and effects on the state and the changes in ecosystem properties [7,8].

The monitoring concept of ecosystem integrity has been the basis of numerous research networks for some time, such as the “Long-term environmental monitoring infrastructures in Europe” (eLTER, [9]), the “Modular Observation Solutions of Earth Systems” (MOSES, [10]) or the Policy European Strategy Forum on Research Infrastructures (ENVRI) [11]. Ecosystem integrity refers to the completeness and balance of ecological systems, where ecosystems are able to maintain their characteristic levels of bio- and geodiversity, structures and functions over time. It encompasses the health and functionality of ecosystems, including the interactions and processes within them that allow for the maintenance of bio- and geodiversity, resilience to disturbances and the provision of ecosystem services that support life, including human life [12]. Key aspects of ecosystem integrity include continuous monitoring of bio- and geodiversity, ecosystem structures, functions and processes and their interactions and changes, and resilience. The ecosystem integrity approach therefore forms the basis of the Ecosystem Integrity Remote Sensing—Modelling and Service Tool—ESIS/Imalys package presented here.

In recent decades, remote sensing (RS) has opened up new and increasingly better opportunities for continuous and objective ecosystem monitoring to detect the status of and changes in their interactions with phylogenetic/genese, structure, taxonomy and function in vegetation diversity [13,14]; geodiversity [3,15]; geomorphodiversity [4,16]; and landscape intensification and urbanisation [17–19] from local to global scale. Recent technological advances in spaceborne RS such as the Hyperspectral Environmental Mapping and Analysis Program (EnMap, [20]), the DLR Earth Sensing Imaging Spectrometer (DESI, [21]) or the GEDI Ecosystem LiDAR [22]), as well as future planned missions such as NASA’s Surface Biology and Geology (SBG) (<https://sbg.jpl.nasa.gov/> (accessed on 1 January 2024), [23]), are largely available free of charge to enable deeper process understanding and accurate estimates of ecological variables.

The pixel reflections in an optical RS image are integral and the result of numerous complex interactions between the light (atmosphere) and the traits of the monitored land and water surface [3,24]. The basis of the spectral trait approach is the spectral variation hypothesis (SVH) approach [25], which assumes that the pixel-to-pixel variability of spectral response in a remotely sensed image is determined by a number of factors, such as the diversity of biochemical–structural characteristics of leaf and canopy traits, functional vegetation traits and their responses through interactions with topography, geodiversity, geomorphodiversity, environmental heterogeneity and land use intensity [25]. As these traits are related to species diversity, spectral texture variations, for example, can be quantified as indicators of plant species diversity [26,27]. Therefore, regions of high spectral heterogeneity in a remotely sensed image may also be regions of high species diversity and ecological heterogeneity, with a range of available ecological niches [25,28]. Thus, traits and their changes (trait variation) are closely linked to structural and functional traits across an ecosystem [29]. Furthermore, traits are proxies and indicators for vegetation vitality [30]

and pressures such as land use intensity and urbanisation [18]. The approach also has the potential to make other connections in the study and management of social–ecological systems [31].

RS technologies can only capture traits and trait variations and their interactions on the land cover and the water surface, so RS and the trait and trait variation approach are crucial for the ESIS/Imalys tool.

In order to use RS data and data products in ecological modelling, it is necessary to derive RS-based indicators. Based on RS data, there are currently two approaches to quantify of structural, taxonomic and functional indicators, namely: (i) the discrete remote sensing approach (patch matrix mosaic (PMM) model approach, derivation of landscape metrics) [32], the best known tool for which is Fragstats [33], and (ii) the continuous RS approach (gradient model (GM) approach, derivation of surface metrics) [34]. Currently, there is no tool or service for hybrid (raster and vector) quantification of structural, taxonomic or functional indicators based on a PMM and GM approach in a simple compact tool package. Although Google Earth Engine allows for the hybrid quantification of indicators, this requires extensive programming on the part of the user. Furthermore, there is currently no GUI implemented in Google Earth Engine that would greatly facilitate the derivation of indicators.

However, for a better understanding of ecosystem processes, the two quantitative approaches for deriving RS indicators, GMM and PM, need to be combined to balance the disadvantages of one approach with the advantages of the other [32]. Therefore, the main innovation of the ESIS/Imalys tool is to create an RS tool that allows for RS data processing, data management, and continuous and discrete quantification of RS indicators in one tool. With the ESIS project (Ecosystem Integrity Remote Sensing—Modelling and Service Tool) we try to put environmental indicators on a clearly defined and reproducible basis. The Imalys software library generates the RS indicators and remote sensing products defined for ESIS.

Therefore, the objectives of this paper are as follows:

- (I) Presentation of the RS tool—ESIS/Imalys.
- (II) To present the RS indicators that can be derived based on the Imalys library.
- (III) Discuss the advantages and disadvantages of the new tool.
- (IV) Demonstrate the applicability of the RS-based indicators by means of several ecological applications.
- (V) Provide an overview of the technical background of the implementation of the Imalys library, data formats and possible graphical user interfaces.

## 2. The ESIS/Imalys Tool for Integrated Landscape Analysis with RS Data

### 2.1. The Aims of ESIS/Imalys Tool

The main innovation of the ESIS/Imalys tool is the creation of an RS tool that allows for RS data processing, data management and, importantly, the parallel quantification of continuous and discrete RS indicators in a single tool. Thus, indicators can be derived simultaneously based on continuous RS indicators (Figure 1a) and, through the segmentation process, discrete zones and zone indicators comparable to the GEOBIO approach [35,36] can be derived simultaneously (Figure 1b). Furthermore, by combining spatial, temporal and spectral RS features, different indicators can be quantified to derive a qualitative and quantitative characterisation of phylogenetic and geogenic traits (Figure 1c,d); structural (Figure 1e), taxonomic (Figure 1f), functional (Figure 1g) and temporal traits (Figure 1h); as well as patterns of vegetation and geodiversity.

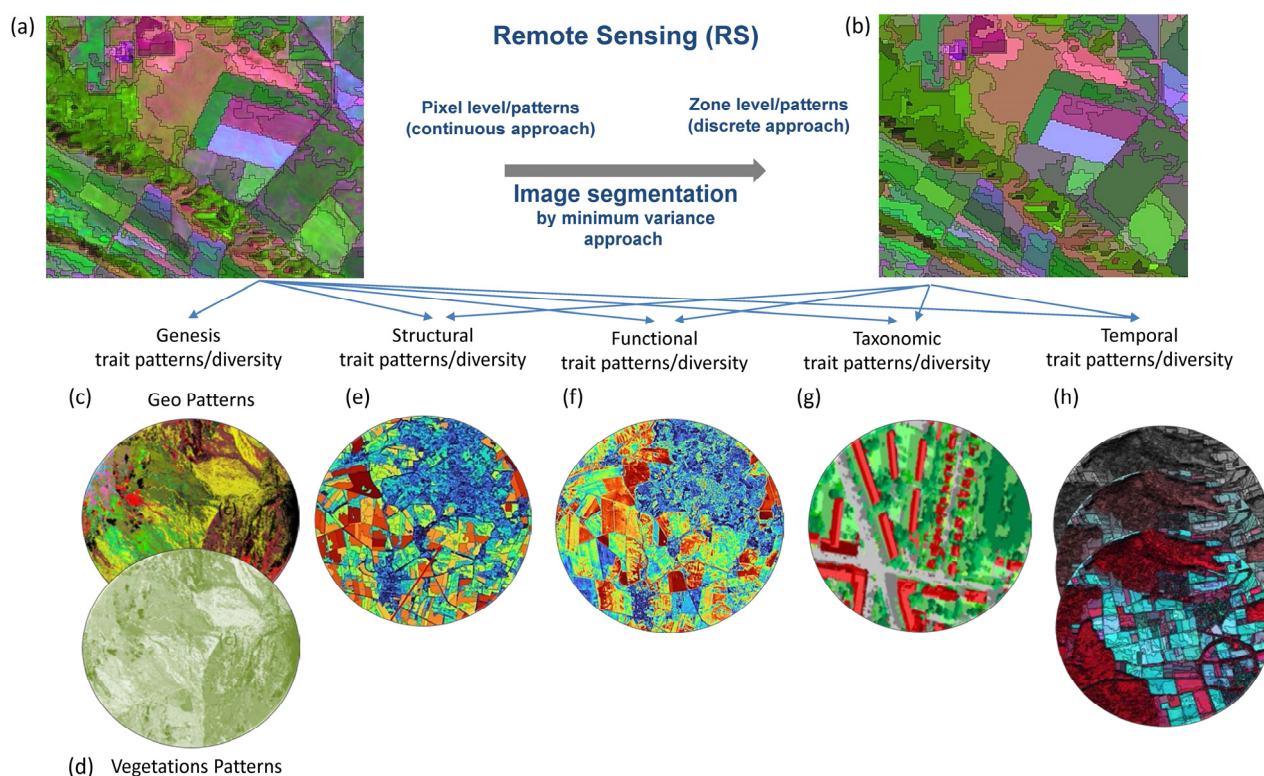


**Figure 1.** Quantitative recording of remote sensing-based indicators at (a) the pixel level and (b) the zonal vector level for quantifying plant and geo-trait diversity; (c,d) phylogenetic plant and geogenese of geodiversity; (e) structural, (f) functional, (g) taxonomic, and (h) temporal trait patterns and their temporal changes.

A summary of the basic functional blocks is given in Figure A1 and Table A1 in the Appendix B. The ESIS software library Imalys contains tools to derive traits from publicly available RS data and/or data products. An appropriate procedure has been implemented for several RS-based characteristics. The tool has a modular structure, i.e., all methods and functions can be combined in a modular way. The ESIS/Imalys tool is open to any kind of RS data source as well as to new procedures and methods to be implemented by the user.

## 2.2. Technological Foundations of the ESIS/Imalys Tool

The combined ecosystem integrity, trait, and RS approach builds on initial developments of the software library “Imalys” [37–40]. Imalys is a software tool with a collection of functions and methods that can be used in a modular way for the complete analysis and derivation of remotely sensed indicators. Imalys is written in the Free Pascal programming language on Linux. Programme developers need the Free Pascal Component Library and the Free Pascal Runtime Library. The source code is available under an Open Source license (GPL). The Imalys source code is open source and is hosted and maintained in the Helmholtz Codebase. There is also complete documentation of all methods, functions and derived indicators described in the openly available Imalys manual. All indicators derived in Imalys are available in raster and/or vector format. The spectral RS-based features of ESIS are defined characteristics of a landscape and its terrestrial and aquatic surface. They are visualised using the QGIS front-end.

Imalys is composed of different blocks. Figure A1 (Appendix B) provide an overview and description of all current tools in the Imalys workflow (see also the Imalys documentation [40]). Imalys provides processes for the import and export of raster and vector data. About 50 raster and 20 vector formats can be read and written. The procedures can be used for all airborne and spaceborne RS sensors (RGB (red green blue), CIR (colour infrared),

HSP (hyperspectral), MSP (multispectral), TIR (thermal infrared), RADAR (radio detection and ranging) and as data products with any spatial resolution from cm to km.

### 2.3. ESIS/Imalys Tool and Processing Overview

Most of the methods and analyses implemented in ESIS/Imalys are also available in commercial software such as ERDAS, ENVI, ArcGIS or QGIS. The key to this new tool is that all the necessary commands and parameters are bundled and made available in a modular process and tool that contains all the sub-steps necessary for the continuous and discrete derivation of RS indicators in one package. The tool solves this requirement by combining a “process list” with names and parameters of all necessary steps from data extraction to the final product and a “variable list” with varying input parameters. Imalys automatically repeats the processes for each set of variables transferred. All input and output products are compatible with each other, so the user can easily modify or add to a given process chain. Figure 2 gives a brief overview of the main blocks of implemented processes, methods and different indicators (VIII-1—VIII-4) that can be used by the user with the help of the Imalys library (see also Figure A1 (Appendix B) and Table A1 (Appendix B)).

- Figure 2 (I) Data import and processing: The process selects spatially and temporally suitable RS data from any collection of provider archives (e.g., Google Earth Engine), checks the image quality within the given frame, extracts the selected bands from the archives, calibrates the raw data for TOA reflectance, reprojects all sections if necessary, combines sections from different tiles of the provider, generates a short time series and forms a data product with the most frequent values for each pixel for the selected period (see also Figure A1 (Appendix B) and Table A1 (Appendix B)).
- Figure 2 (II) Statistical reduction of RS data: Here, the user can find methods for the statistical reduction of large RS datasets such as Mean, Median, Principal and Replace Image Bands (see also Figure A1 (Appendix B) and Table A1 (Appendix B)).
- Figure 2 (III) Management: The user can use RS data management methods such as Stack, Merge and Organise RS data (see also Figure A1 (Appendix B) and Table A1 (Appendix B)).
- Figure 2 (VI–VII) Pixels, zones, classes, objects: The creation of pixels, the segmentation of zones and the extraction of classes and objects are described in detail in Sections 2.3 and 3.5 (see also Figure A1 (Appendix B) and Table A1 (Appendix B)).
- Figure 2 (VIII-1) Indicators by kernel process: This part is the pixel area of Imalys where grid-based indicators—which are Normal, Inverse, Deviation, Roughness (Rao’s Q index), Entropy, Diversity, Proportion, Relation, Diffusion, Values, Lowpass and Laplace—are calculated using the kernel method. Some examples of kernel-based indicators are described in Section 3.3 (see also Figure A1 (Appendix B) and Table A1 (Appendix B)).
- Figure 2 (VIII-2) Indicators by zone: Deriving zonal indicators by Dendrites and Cell Size. Some examples of indicators by zones are described in Section 3.4 (see also Figure A1 (Appendix B) and Table A1 (Appendix B)).
- Figure 2 (VIII-3) Raster indicators for zones: All indicators generated on the basis of the kernel process can be quantified here for each zone. The indicators are Normal, Inverse, Deviation, Roughness (Rao’s Q index), Entropy, Diversity, Proportion, Relation, Diffusion, Values, Lowpass and Laplace. Section 3.4 describes some examples of kernel-based indicators derived for zones (see also Figure A1 (Appendix B) and Table A1 (Appendix B)).
- Figure 2 (VIII-4) Time series indicators: RS time series indicators are Regression, Difference, NirV, NDVI, EVI, LAI, Time Series. In addition, time series can also be generated for time series indicators by zone and time series grid indicators for zones. Examples of time series indicators can be found in Section 3.2 (see also Figure A1 (Annex) and Table A1 (Annex)).
- Figure 2 (IX) Export: Export of raster data, raster-based indicators, classification results and objects; zones can be exported and later imported and managed in QGIS or

another GIS as a vector layer with zone indicators and tables (see also Figure A1 (Appendix B) and Table A1 (Appendix B)).

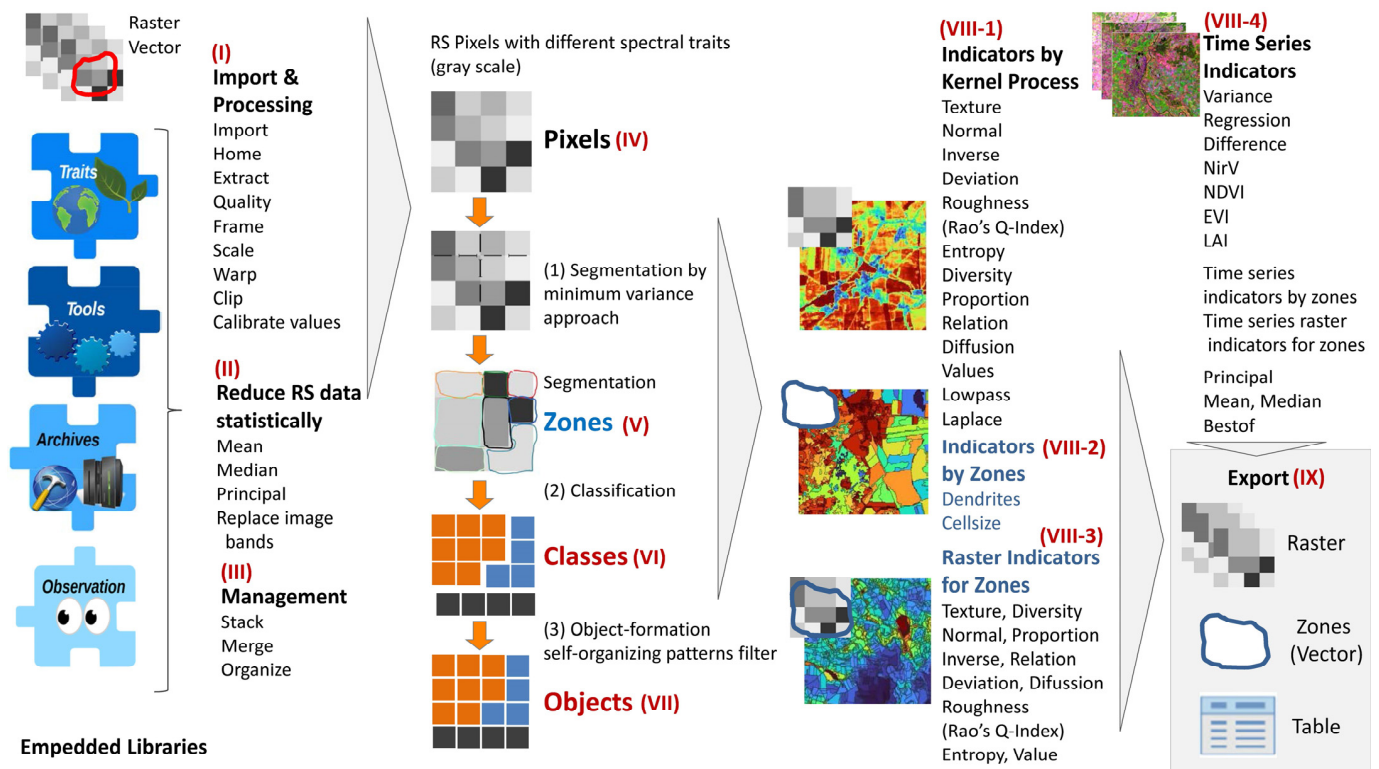


**Figure 2.** Flowchart of the ESIS/Imalys tool: the managing, processing and derivation of different indicators.

#### 2.4. Creation of Pixels, Zones, Classes and Objects

In the derivation of zones, classes and objects, which are in different stages within Imalys, pixels can be considered as “square zones”. Their shape and size are always the same. Pixels differ in the characteristic and density of spectral traits in the different RS channels (spectral combinations). Pixels with similar traits are segmented into zones based on the minimum variance approach. Zones are contiguous areas of arbitrary shape and size that have broadly similar traits in the image. The spectral characteristics as well as the shape, size and position of each zone are classified. The classes can be formed automatically (clustering, unsupervised classification) or by training on in situ data (supervised classification). Classes have the same shape as zones but only have one feature (discrete), their class ID. Object formation is a self-training pattern filter based on a neural network approach. The class features in this case are the lengths of the boundaries to the different classes of neighbouring zones. Objects are contiguous areas of different zones. The zones in an object form typical spatial patterns of different classes, where the classes themselves and the length of the boundaries between the different classes are decisive.

##### 2.4.1. Pixels

RS pixels can be thought of as “small square zones”. Their shape and size are always the same and depend on the spatial resolution of the imported RS data (e.g., aerial photo: 20 cm; Landsat 4–9: 30 m). Thus, pixels only differ to each other in terms of their density, spatial distribution or trait variations within the different RS channels. The “Pixel” module in Imalys provides tools to reduce image stacks using statistical methods, such as median or variance, to create time series and derive trends, or to construct spectral indicators such as the near-infrared vegetation index (NirV). The second part of the Pixel module consists of tools to collect information about the local pixel environment using a user-defined kernel.

Kernels can enhance image contrast, such as a Laplace transformation, or extract local patterns based on Rao's diversity [41] (see also Section 3.3). A description of all raster-based indicators implemented in Imalys so far can be found in Figure A1 (Appendix B) and Table A1 (Appendix B).

#### 2.4.2. Zones

Neighbouring pixels with similar traits such as reflectance, texture, moisture, chlorophyll or water content or others are divided up into contiguous polygons (or zones). Imalys uses the variance of neighbouring pixels to separate the zones. The algorithm determines the boundaries between the zones in such a way that the variance of the pixels within the zones is minimised. In contrast to approaches based on gradient descent or a watershed (e.g., eCognition), the variance was found to be comparatively robust to noise and to random fluctuations in the image data. Narrow or dendritic shapes such as watercourses or roads are mapped coherently, even without clear boundaries. A user-defined threshold controls the average size of the zones with the size of the zones depending on the number of pixels per zone and on their spectral heterogeneity. Thus, large zones are more homogeneous, while small zones are more heterogeneous. The zones contain not only properties derived from the mean values of the raster indicators but also properties based on morphological indicators such as shape, size, entropy, diversity or dendrites (see Table A1, zonal indicators, Appendix B). Figure 3 shows zones for the Leipzig region, delineated as regions with the smallest possible deviation within the zones compared.

### Zones

Zones are delineated as regions with the smallest possible deviation within the zones compared with the mean deviation of the whole image. The process can be stopped at intermediate stages.

- ▶ Zones: Delineated landscape elements
- ▶ Image superimposed by zones borders
- ▶ Landsat 8/9
- ▶ Bands: 5 · 4 · 3
- ▶ Calibrated to TOA reflectance
- ▶ May ... August, 2018 ... 2023
- ▶ Median of all accepted images
- ▶ City of Leipzig, Germany

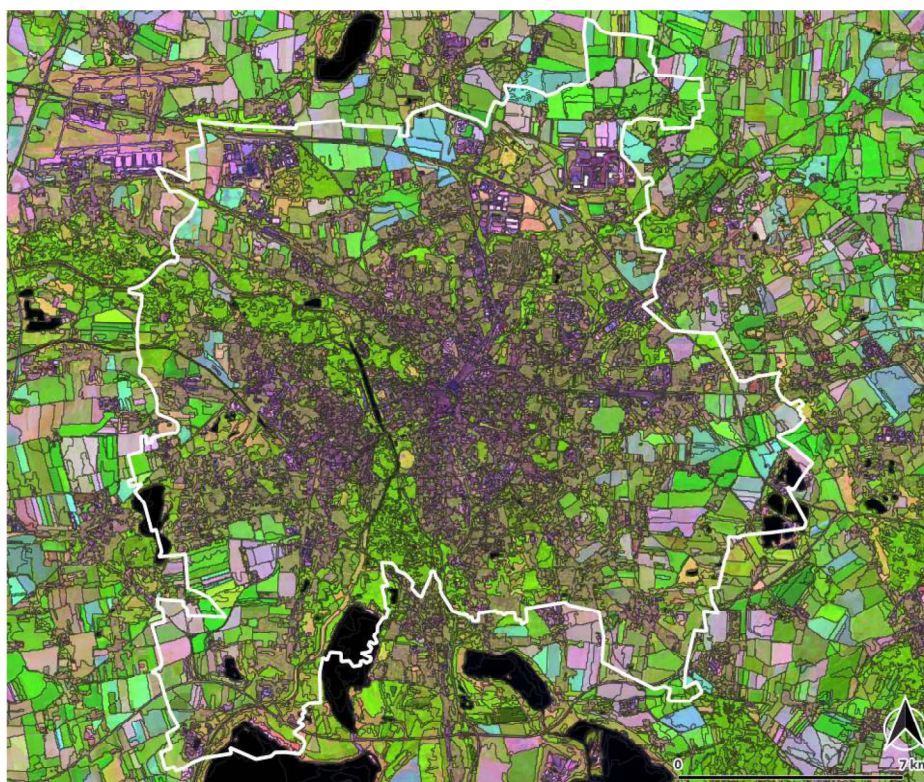


**Figure 3.** Zones are delineated as regions with the smallest possible deviation within the zones compared to the mean deviation of the entire image. The process can be stopped at intermediate stages. Zones delineated with Landsat 8/9 time series data from 2018–2023, city (white line) and region of Leipzig, Germany.



### 2.4.3. Classes

Spectral traits as well as the shape, size and location of individual zones can be aggregated or classified into classes. Pixels can be classified by an unsupervised classification process (self-calibrating pattern detectors, without training, clustering method) or by training on in situ data (supervised classification) (see Figure 2). Zones can be classified as pixels. All pixels within a zone are assigned to the same class. Unlike pixels, zones can also use shape and size features of the zones for classification. Classes are raster data that have the same shape as zones, but they are assigned only one discrete feature, their class. The number of classes can be selected in Imalys. The Classes module provides additional tools for using training patterns from in situ data, comparing classification results with predefined GIS maps and tracking outliers in space and time.

### 2.4.4. Objects

Imalys also offers the possibility to combine different zones into larger “Objects” (see Figure 2). Objects are the result of a further classification using only the length of the boundaries between different zones. Object formation is a self-organising pattern filter based on the neural network approach, which is based on the perceptron principle. Objects are combinations or patterns of different zones. Object formation in Imalys filters the most common patterns from the image and returning a pattern definition. The process captures all boundaries between two pixels and enters the class of zones from each pair of pixels into a table. Of the many possible combinations between two zone classes, only a few are really common. Frequent combinations are thus formed into objects (see Figure 2). The process is designed so there is no limit to the number of zones that can be linked, nor the number of classes that can form a pattern definition. Objects can consist of only one class. River courses, for example, have boundaries with many land cover types and are non-specific. The object “river course” is usually only defined by the river itself.

## 3. Remote Sensing, Data Processing, Analysis and Management in ESIS/Imalys Tool

Block (1–3) is the pixel area containing methods for extracting, combining and pre-processing image data from the compressed archives of the providers (see Figure A1 (Appendix B)). The sequence of methods applied and the resulting results within Imalys can be used by the user in a modular way. The RS data can be cropped or merged, the coordinate system can be changed, and the pixel size can be adjusted. In addition, raw RS data can be calibrated to reflectance or other defined values such as radiation or heat. Internally, all images are stored in ENVI format, which allows for Imalys to meet the requirements of the European Space Agency (ESA). All descriptions of the methods, functions and statistical formulae from Block 1 can be found in Table A1 (Appendix B). In order to derive raster-based indicators, Imalys allows for new channel combinations to be generated from the raw RS data through pixel-based processes. Imalys contains three groups of routines, namely, “raster-based indices”, “time series analysis” and the application of “kernel methods”. These are used to modify the RS pixels, combine them with each other and derive indicators.

### 3.1. Grid-Based Indicators

Raster-based indices are derived by combining of different spectral channels (e.g., frequencies, spectral band information, etc.) from an RS dataset, to derive new properties, such as a vegetation index (near-infrared vegetation index (NIRv) or the leaf area index (LAI) (see Figure A1 (Appendix B) and Table A1 (Appendix B)). The near-infrared vegetation index (NIRv) is calculated as the product of near-infrared radiation and the normalised difference between the red and the near-infrared radiation. The calculation follows the most common NDVI definition but performs better at mapping areas with sparse vegetation [42]. Vegetation indices have been introduced to estimate the proportion of the landscape covered by vegetation, where the result depends on the photosynthetic activity of the vegetation in question. Vegetation indices attempt to quantify the photosynthetically

active radiation (PAR) as a measure of plant metabolism. About 20 different approximations are described (see also Table A1, Appendix B). Due to the modular concept, a large number of other raster-based indicators can also be derived from different band combinations.

### 3.2. Remote Sensing Time Series Indicators


Time series compare the same spectral RS channels from different points in time to identify outliers, changes or temporal trends. Within Imalys, the three methods, “Variance”, “Regression” and “Difference”, can be used with the routine “Reduce time series” to search for and quantify temporal changes, trends or temporal outliers. At mid latitudes, there are distinct seasonal periods. Seasonal changes in landscapes are often more obvious than changes over the years. In order to represent typical features of a landscape or to look for outliers, the season of the photographs should be taken into account in the analysis. The “median” (see Figure A1 (Appendix B) and Table A1 (Appendix B)) is not applicable when large natural or anthropogenic changes, such as harvesting, occur. Images from the same seasons but different years provide images with typical characteristics for the selected period. The use of filtered time series over longer periods is therefore a goal when applying the “median”. The images must be free of errors in every single pixel. The space-based RS missions Landsat 5–9 (1985–date in orbit) or Copernicus (2015–date in orbit) allow for the use of continuous time series of up to 38 years. The extent and direction of periodic change in landscapes is a specific feature of many landscape types. Settled areas show only small periodic changes, while deciduous forests show clear but regular fluctuations. Arable land, on the other hand, shows an indication of high and irregular changes over the years, which can be caused by sowing, harvesting and phenology as well as stress events (drought, windthrow, pesticide use, management). Permanent grassland, in turn, can be described by its periodicity.

Variance describes how large the change is and thus identifies typical fluctuations, while the regression describes whether there is a direction of landscape change or whether this direction cannot be clearly identified. Both methods require at least three different time periods or states. The variance command determines the variance in individual pixels based on a standard distribution for all bands of the source. In the case of multiple image stacks, the Variance method determines the variance for each band individually and returns the result as a multispectral image of the variances. The result can be further reduced to a single-band image with the first principal component of all bands using “Principal Components” (see Figures 4 and A1 (Appendix B) and Table A1 (Appendix B)).

The Regression method, on the other hand, determines whether a value is increasing or decreasing over time, even if the values fluctuate greatly. For this purpose, the regression is calculated separately for each channel, as it may be different for each channel. If the regression is the same for each channel, the image is colourless (black to white: a strong decrease to a strong increase). The colours show differences in the regression between channels (see Figure 5). The blue-grey on the croplands shows that the regression has changed somewhat but in the same direction in all channels. Strong colours show large differences in the regression between channels (forest). The results are two images (variance and regression) with 6 channels each, derived from Landsat 5 channels 1–5 and 7. They show the variance and regression for each channel individually. The variance shows how much the change was, while the regression shows whether the change had a direction or was just irregular. The channel combination 5-4-3 is used for both plots as it contains the most information. The info function in QGIS and the graph are used for display. Such results can be used as features and then classified.

## NIRv: Variance in Time

The square of the standard deviation is called “variance”. In this case the variance in time reaches 0.02 or 45% deviation from the mean of the NirV index.

- ▶ Time course 2018...2023
- ▶ NirV plant metabolism index
- ▶ Season: May...October
- ▶ Values: 0.0.....0.032
- ▶ Colors: 
- ▶ Sensor Landsat 8/9
- ▶ Calibrated to TOA reflectance
- ▶ City of Leipzig, Germany



**Figure 4.** The indicator Variance is calculated separately for each channel. In the result, each channel gives the median of a Landsat 8/9 time series from 2018–2023. The square of the standard deviation is the variance. In this case, the time variance reaches 0.02 or 45% deviation from the mean of the NirV index. Landsat 8/9 time series, May to October from 2018 to 2023, Leipzig region, Germany.


### 3.3. Kernel Processes for Estimating Raster-Based Indicators

Kernel approaches are used to quantify the local environment of each pixel through a moving window approach for spectral similarities or differences, patterns, heterogeneity, roughness or contrast changes with respect to its environment. Thus, the kernel processes assign a new value to each pixel in each spectral band through the moving window approach. The value is determined from a small window (window size can be selected by the user) around a central pixel of the window (kernel). In ecology, land surface diversity is defined as the probability that different traits of bio- and geodiversity can occur in one place. Spectral diversity or texture has traditionally been used in RS as a measure of ecological diversity. Indicators for quantifying and inferring landscape diversity from imagery data are therefore a major focus in the development of the Imalys method. Imalys provides a set of methods to quantify texture, roughness, entropy, diversity or homogeneity as well as spatiotemporal changes to the imaged structures. The entropy and roughness methods are described in more detail below.

Rao’s entropy (diversity) based on classes. The Entropy indicator or Rao’s class diversity captures the number of class differences and class similarities for all pixel combinations within a given kernel. The number of different class combinations is scaled by the spectral differences between classes. Entropy requires a classification of the images to work. The easiest way to obtain this classification is to invoke Mapping. Alternatively, Entropy can use an existing classification. Entropy returns the range of landscape classes within a given core and ignores small landscape differences represented by the same class, providing a more abstract level. Rao’s approach is insensitive to the distribution of pixels within the kernel. A checkerboard distribution of two classes gives the same result as two homogeneous areas with the same classes (see also Figure A1 (Appendix B) and Table A1 (Appendix B)).

## NIRv: Regression in Time

Regression is used to estimate dependencies between different parameters. In this case the NirV index shows a linear increase (orange) or decrease (blue) up to 0.2% a year.

- ▶ Time course 1984...2022
- ▶ NirV plant metabolism index
- ▶ Season: May...July
- ▶ Values: -0.002.....0.002
- ▶ Colors: 
- ▶ Sensor Landsat 4/5...8/9
- ▶ Calibrated to TOA reflectance
- ▶ Region Leipzig, Germany

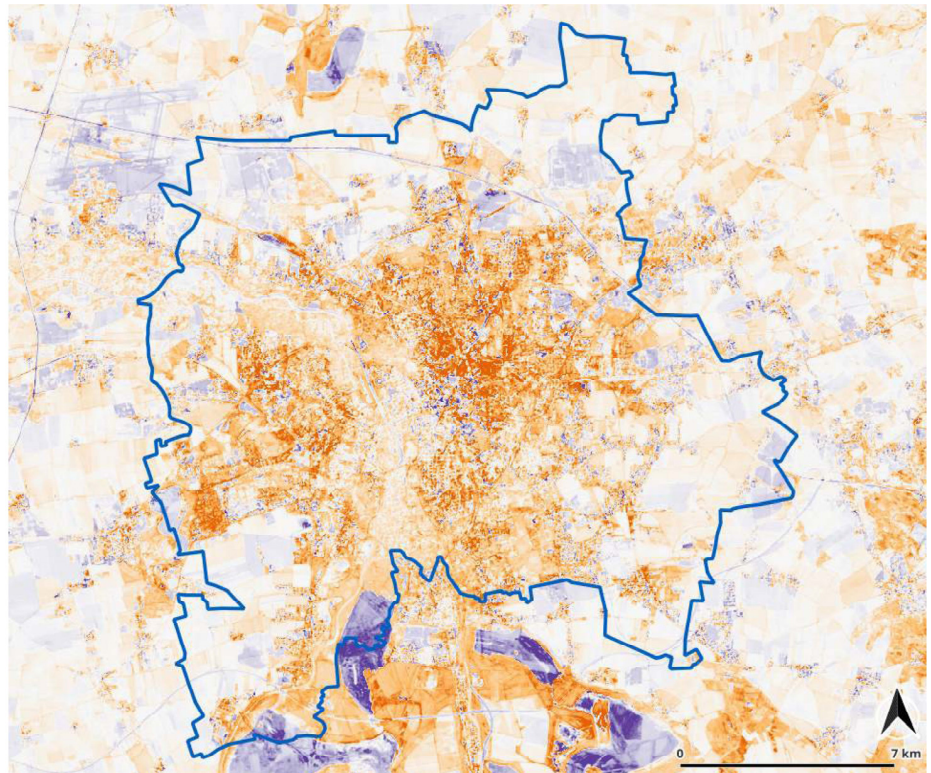


**Figure 5.** The indicator Regression is calculated separately for each channel. In the result, each channel gives the median of a Landsat 8/9 time series from the months May–July from 1984 to 2022. Regression is used to estimate dependencies between different parameters. In this case, the NirV index shows a linear increase (orange) or decrease (blue) of up to 0.2% per year. Regression values may be positive or negative. Medium grey (settlements) indicates values around zero, while dark colours indicate a decrease and light colours an increase in their spectral range. The homogeneous colour of agriculture represents high control–high land use intensity. Landsat 4–9 time series, months May to July from 1984 to 2022, Leipzig region, Germany.

Roughness (Rao's Q Index) based on pixel analysis. Roughness (Rao's Q index) or Rao's diversity is based on the analysis of pixels. Rao's Q is the expected difference in reflectance values between two pixels drawn at random from the set of evaluated pixels. Similar to the Texture indicator, Rao's approach evaluates the spectral difference of individual pixels, but compares not only adjacent pixels, but all pixels within the kernel. Unlike the classical Texture or Normal indicators, Roughness is insensitive to the spatial distribution of pixels within the kernel (see also Figure A1 (Appendix B) and Table A1 (Appendix B)). Roughness provides a measure of landscape diversity based on pixel differences within a given kernel. Similar to Entropy, any distribution of a given set of pixels will produce the same result [41,43,44] (see Figure 6c and Table A1 (Appendix B)).

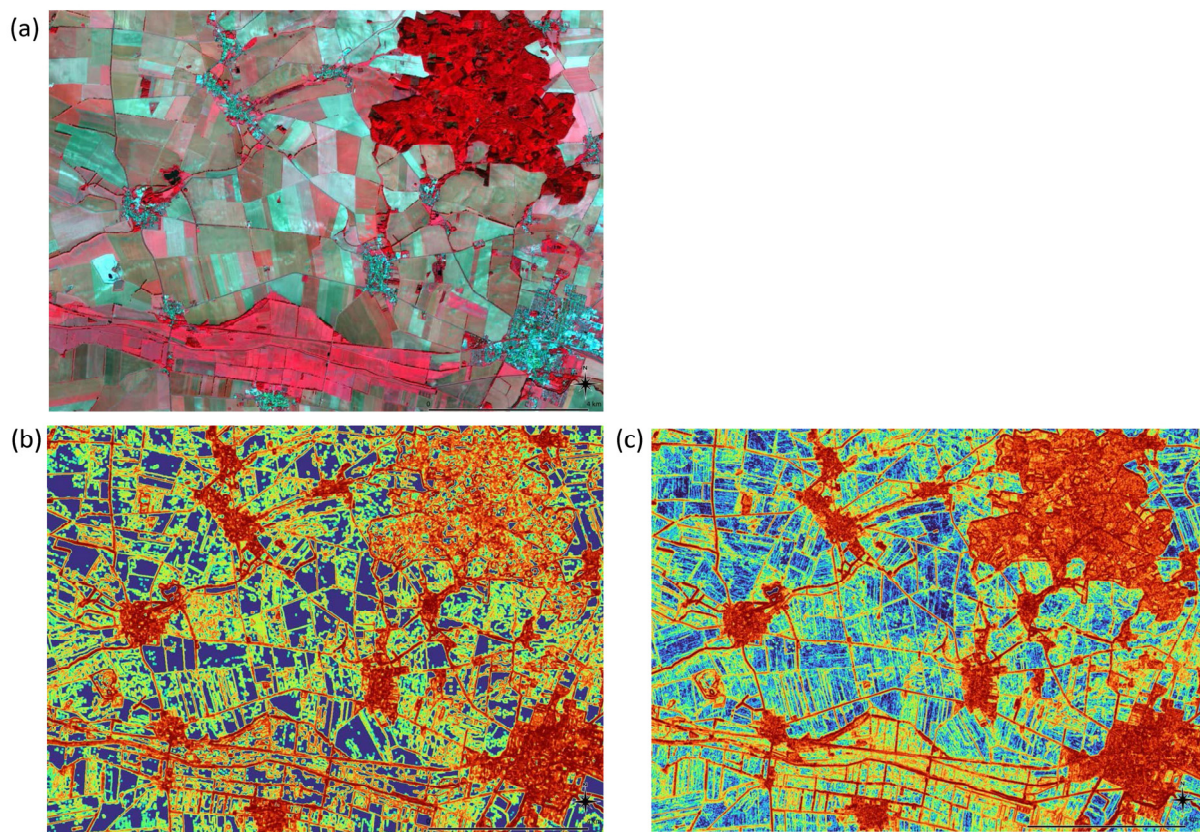


**Figure 6.** (a) Satellite image, infrared colour composition acquisition: May to October bands 8-4-3, Sentinel-2, calibrated for TOA reflectance (TOA = top of atmosphere), average of all accepted images during May, June and July, adjusted for annual contribution, years 2017–2021. (b) Rao's  $\beta$ -entropy (pixel-based). Spectral diversity at pixel level is calculated from class diversity, Rao's  $\beta$ -Entropy reflects the distribution and degree of differences in one a value, sampled for a  $5 \times 5$  pixel kernel, all accepted images between 2017 and 2021, bands 2-3-4-8, Sentinel-2, values: 0.0–0.38 (blue–red). (c) Texture (pixel-based), colour equivalent for spectral diversity at pixel level, equalised with normalised Gaussian kernel,  $5 \times 5$  pixels, values reflect local contrast independent of regional features, values: 0.0–0.38 (blue–red).

### 3.4. Indicators by Zone and Raster Indicators by Zone

In order to derive different indicators for each zone, factors of geometry and the distribution of zones in its neighbourhood are taken into account. Some characteristics describe the shape or geometry of individual zones, such as Cellsize (area) or Dendrites (shape), while others describe the connections with neighbouring zones, such as Relation (density of neighbours) or Diversity (spectral diversity) (see Figure 7 and Table A1 (Appendix B)). Dendrites indicates the quotient of the circumference and the size of the individual zones. Both values increase with larger zones, but the size increases faster. Large zones have lower values than smaller zones with the same shape (see Figure 7b). Dendrites have been introduced as a measure of spatial diversity (independent of size). Long and small zones can be quite large, but their role in landscape diversity is similar to that of small zones. Small, thin or dendritic zones have high values, while large compact zones have the lowest values. Diversity or spectral diversity is calculated as the mean principal component of all spectral differences between all pixels in a single zone. This includes all pixel boundaries to neighbouring zones as well as all pixel boundaries within the zone. Differences are calculated from the averages of zones, not individual pixels. Diversity has been introduced for size-dependent spectral diversity. The principal component enhances the contrast of each band. High values indicate small zones and high spectral differences. Small or narrow zones embedded in large zones are highlighted (see Figure 7c). Relation is calculated

as the ratio between the perimeter of the zone and the number of neighbouring zones. Relation is introduced as an indicator of spatial diversity. Large zones and small zones with few neighbours will have high values, while small zones with many neighbours will have higher values. Similar to Dendrites, Relation gives information about the shape and connection of the zones. Zones with many connections could act as corridors for animals and increase diversity (see Figure 7d).

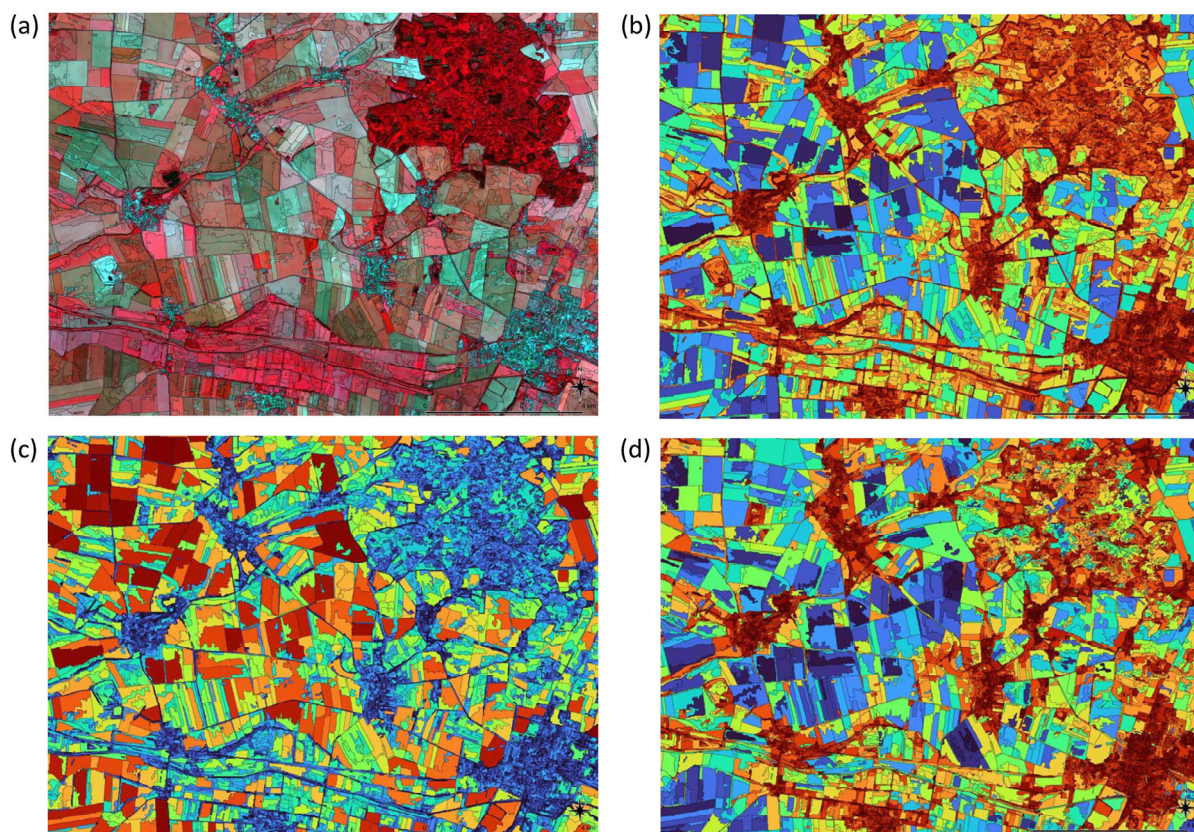


**Figure 7.** (a) Segmentation to create zones, land cover boundaries (borders in black) extracted from all accepted imagery during 2017–2021, regions with homogeneous pixel colour are called Cellsize, about 25,000 polygons in the whole image, May to October, bands 2-3-4-8, Sentinel-2 (10 m). (b) Dendrites—zone indicator, colour equivalent for the quotient of the perimeter and the size of individual cells, values: 0.05–1 (blue–red). (c) Spectral Diversity (cell property) colour equivalent for the principal component of all spectral differences to all neighbouring cells, values: 0.0–3.1 (blue–red). (d) Relation, colour equivalent for the quotient of the cell perimeter and the number of neighbouring cells, values: 0.12–68 (blue–red). For a more detailed explanation of the indicators see Table A1 in the Appendix B.

In addition to the vector-based indicators of the zones, raster-based indicators can also be derived for each individual zone. Thus, by averaging in Imalys, all raster-based indicators such as the Variance, Regression or raster information determined by kernel processes can be determined for each zone. Using features, additional image data can be applied as new attributes to existing zones.

### 3.5. Classification Approach

Ordering image data into clusters: Imalys implements a self-learning classifier to group spectral, spatial and temporal dependent features into classes. In the simplest cases, the template is an image, and the spectral features of the individual image pixels are sorted into clusters. The number of clusters is arbitrary and other parameters are not required for calibrated image data. If images of the same region are available from different years

or seasons, the temporal change can be used as a class feature. To do this, the images need only to be combined into an image stack. Different sensors can also be combined in this way.

Make location-based data comparable: Unusual imagery, such as microwaves or wind speed, has its own range of value. If it is to be compared with spectral data, its value range must be adjusted. The classifier does not distinguish between the origin of different features; it only compares the values of the features. If the values of a feature are unusually large, then they will dominate the results. Features with unusually small values will not be effective. The same applies if, for example, values with a Poisson distribution are to be compared with normally distributed values. Imalys implements routines to make values and distributions more comparable.

Imalys implements a process that combines zones into higher-level “objects”. These objects are made up of zones with different characteristics. Their characteristic feature is the spatial combination or pattern of the different zones in the object. Such objects can be grouped into clusters. This is carried out by first creating clusters of different zone types. Then, the spatial combination of different zone types is sorted into higher order of clusters. Imalys implements a routine that only requires the number of result classes. The object formation only uses the frequency of contacts (common boundaries on the pixel level) between the different zones. It is structurally similar to a neural network based on the perceptron principle. The result is a classifier that can map spatially structured objects and, if necessary, their change over time.

#### 4. Possibilities and Limitations of the ESIS/Imalys Tool

The ESIS/Imalys tool is a standalone application that runs in a server environment or on a PC with a Linux operating system. The Imalys code is open source and developers can integrate parts of the programme into their own software. Imalys is designed to process and manage large amounts of data as automatically as possible. For a process chain example, see Figure A1 in Appendix B. Surface and modelling tools (e.g., model toolboxes) are not flexible enough for this. For example, applications with a graphical user interface (GUI) can occupy considerable amounts of RAM. Imalys, on the other hand, only requires memory for RS data. The user controls Imalys by means of commands and parameters. These are given in the form of a list, the structure of which is simple. The selection of the order of commands is modular and is the sole responsibility of the user. By using Imalys, the user gains time and flexibility in deriving RS-based indicators. A list of commands and parameters can contain variables (see Table A1, Appendix B). Imalys can then repeat the command list as often as required with automatically modified inputs. Unlike a software interface, commands and parameters must be set correctly. Logical errors will be executed, and missing inputs will lead to empty results.

Imalys was developed to process satellite images as automatically as possible. New projects require the addition of new landscape indicators based on largely homogeneous areas (zones). Imalys combines both functions in a single software package and command set. When large or numerous areas need to be processed identically, Imalys requires no intermediate steps or interactions.

In addition, Imalys provides new indicators of the diversity and spatial connectivity of different areas. With Imalys, each RS time series spectral channel is stored in a layer stack. This means that any user can easily quantify known or user-defined indicators. Finally, Imalys seeks to bring together information of all kinds under a common nomenclature and make it comparable. Traditional in situ measurements are very accurate, but they are selective and mostly random. Stationary measurements with a long time series are also often only possible at certain points. RS has recorded every location on earth for 5 decades, so Imalys can draw on long continuous RS time series. RS records traits and trait variations. Traits exist at all spatial and temporal scales, allowing for the use of RS to study standardised and comparable indicators at all monitoring scales.

## 5. Possible Applications of the ESIS/Imalys Tool

The ESIS/Imalys tool is particularly important because it is based on the spectral trait approach, and therefore continuous raster trait data of the land surface, and is not limited to the classification of discrete landcover classifications. This means that the internal diversity and characteristics of land surface and landscape structure can be better quantified [32]. This allows for more appropriate indicators to be derived for subsequent modelling at both pixel and zonal scales. However, all applications are based on the same basic principles, but also on limitations resulting from the use of RS data. Limitations to the quantification of indicators using Imalys arise from, among other things, the characteristics of the RS sensors (spatial, spectral, temporal and directional resolution), as well as the density, distribution and characteristics of the land surface traits to be recorded [4]. This section presents examples of possible applications that can be realised with Imalys.

### *Example 1: Monitoring landscape diversity*

The diversity of a landscape is a key indicator of its stability and important ecosystem functions. For example, pollinator insects are more abundant in diverse landscapes than in homogeneous regions. In addition, genetic exchange is often linked to suitable corridors. Several indicators of diversity can be quantified using Imalys. For example, (I) the heterogeneity of areas can be quantified locally at the level of individual areas (zones), and (II) indicators such as area size or shape of the different zones can be recorded at the regional level in order to quantify the density of different area types and their diversity at the next higher scale. In addition, diversity (III) can be quantified structurally by analysing the frequency and quality of contacts between zones in order to make statements about the connectivity and isolation of different biotope types.

The Deviation indicator reflects the (spectral) diversity for individual zones based on the pixel Rao's diversity index (see Table A1, Appendix B). However, Rao's diversity uses variance rather than texture to assess the spectral diversity of landscape structures. Variance is insensitive to the spatial distribution of pixels within the kernel. As a result, Deviation shows high values for small-scale and varied landscapes with high spectral pixel diversity. An increase in the Deviation value indicates an increase in spectral diversity or an increase in the internal fan diversity of the landscape.

Analogous to Deviation, the diversity shows the spectral differences between adjacent zones in a pixel grid. The spectral diversity between zones is calculated as the Euclidean distance of all spectral grid features between the central zone and all its neighbours. Similar to the indicator Relation, the spectral diversity measures the diversity in a complex of a central zone and all its neighbours. As the zones can vary considerably in shape and size, the greater the spectral difference and the longer the boundary to the central zone, the greater the contribution of each neighbouring zone to the overall result. Lower spectral diversity is an indicator of landscape monotony at the zone level, as is the case with agricultural areas consisting of many monocultures.

### *Example 2: Monitoring landscape structure and landscape fragmentation*

Numerous studies confirm that landscape structure has a strong influence on water quality, e.g., [45–47]. RS time series can be used to derive indicators in Imalys that are important for assessing landscape structure and fragmentation.

For example, the normalised texture (indicator Normal) can be quantified in Imalys like a normal texture, but using the ratio of the difference in brightness to the brightness of all pixels involved within each zone (see Table A1, Appendix B). Thus, in bright areas such as industrial zones, the differences in values are large, even if the relative differences are small. The opposite is true for dark forests. The Normal indicator thus represents the (spectral) diversity or heterogeneity at pixel level, which is independent of the brightness of the objects represented. The indicator is high for varied surfaces, with settlements usually having the highest values. An increase in the Normal indicator therefore indicates a structured landscape with a high degree of heterogeneity.



The increase in the Cellsize indicator is an indicator of the increase in the area size of the land cover classes analysed, such as agricultural or forest areas. Cellsize describes the area of the zones. High values indicate low diversity and possibly monocultures. Comparatively large, machine-friendly areas are also an indicator of higher intensity of use of agricultural land.

The indicator Dendrites gives the ratio of the extent and size of individual zones. Dendrites is comparable to the Shape Index indicator of the Fragstats tool (V.4.3) [33]. Perimeter and size increase with larger zones, but size increases more rapidly. Large zones have lower dendritic values than smaller zones of the same shape. This indicates that the landscape structure is characterised by large compact zones of landscape structure. Low values are an indicator of low patch or zone diversity, and thus a lower potential for genetic exchange between species.

The indicator Relation was quantified as a measure of the density of contacts with other zones. Unlike the Dendrites indicator, Relation does not evaluate individual zones, but the complex of a central zone and all its neighbours. The Relation indicator is calculated as the ratio between the number of neighbouring zones and the size of the central zone. Like Dendrites, Relation provides information about the shape and connectivity of the zones. As the Relation indicator is comparable to the Dendrites indicator, its assessment that the landscape structure is characterised by large compact zones of landscape structure is also comparable.

### *Example 3: Monitoring land use intensity and its impact on ecosystem functions*

Land use intensity is a key driver of many changes and disturbances in ecosystem functioning. However, to date, there are few meaningful indicators for quantifying LUI. The Imalys indicators can make a valuable contribution. For example, the indicators NirV-Mean and NDVI-Mean can be derived from Landsat time series for summer (May to July) and NirV2 and NDVI2 for autumn (August to October). NirV has been developed as a proxy for photosynthetically active radiation (PAR), which is proportional to the metabolic rate of vegetation, whereas NDVI is more a measure of the density of green vegetation. An increase in NirV indicates increased vegetation metabolism, which can be caused by higher CO<sub>2</sub> concentrations in the air. The measured values correspond to those of the Global Monitoring for Environment and Development (WHO). Similarly, an increase in metabolism can be caused by an increase in fertilisation.

The quantification of land use intensity and its effects on ecosystem functions can be performed by calculating the variance in indicators NirV and NDVI, NirV- and NDVI regression, using Landsat time series data. The variance indicator quantifies the variance in individual pixels based on a standard distribution for all RS bands. A decrease in the NDVI variance indicator can be explained by having been set aside or an increase in development and thus a change in the proportion of vegetation.

The Regression indicator, in turn, provides the regression of the individual pixels of all bands on the standard deviation. Regression uses the temporal distance of the images from the metadata of the images. Similar to Variance, Regression calculates the regression for each band separately if multispectral images are available, and outputs a multispectral regression. A strong increase in the NirV regression indicator indicates a higher CO<sub>2</sub> concentration in the air or is an indicator of an increase in the use of fertilisers in agriculture. Imalys also allows for the use and quantification of indicators from TIR Landsat time series data. Using TIR, important functions in urban landscapes such as heat islands or changes in evapotranspiration can be assessed as indicators of climate change and increased soil aridity in landscapes.

Further, more applications are possible:

- Monitoring the intensity of urban land use.
- Assessment of the hemeroby or naturalness of landscapes.

- Monitoring vegetation diversity and geodiversity by deriving indicators to quantify genetic diversity, trait diversity, structural diversity, taxonomic diversity and functional diversity.
- Monitoring of species distribution (fauna and flora).
- Monitoring of water quality and its drivers such as LUI.
- Monitoring of vegetation vitality (e.g., bark beetle infections).
- Monitoring of the ecosystem and its processes and changes.

## 6. Summary and Outlook

Climate change, land use intensification, biological invasions and loss of biological and geographic diversity are causing rapid environmental changes with local- to global-scale impacts. There is therefore an urgent need for operational monitoring and observation tools and services that can monitor and quantify aspects of changing impacts on ecosystem functions, vegetation and geodiversity, and landscape resilience. In order to use RS data and products in ecological modelling, RS-based indicators need to be derived. Currently, there are no services available to quantify both raster and vector-based indicators in a “compact tool”. Therefore, the main innovation of ESIS/Imalys is to create an RS tool that allows for RS data processing, data management and continuous and discrete quantification of RS indicators in one tool. With the ESIS project (Ecosystem Integrity Remote Sensing—Modelling and Service Tool), we try to present environmental indicators on a clearly defined and reproducible basis. The Imalys software library generates the RS indicators and remote sensing products defined for ESIS.

The ESIS/Imalys tool has a modular structure, so that users can combine different modules or create their own routines and methods, depending on the question at hand. Despite the integration of large-scale RS data, the software can be operated from a PC, as the processing and derivation of indicators has been greatly optimised. Imalys is written in Free Pascal. The Imalys source code is open source (GPLv3), hosted and maintained in the Helmholtz Codebase: <https://doi.org/10.5281/zenodo.8116370>. There is also a complete documentation of all of the methods, functions and indicators derived, which can be found in the openly available Imalys manual [40].

This document provides an overview of the functionality of the Imalys tool. An overview of the technical background of the implementation of the Imalys library, data formats and possible graphical user interfaces is given. Examples of RS-based indicators derived using Imalys at pixel level and at zone level (vector level) are presented. Furthermore, the advantages and disadvantages of the Imalys tool are discussed in detail in order to better assess the value of Imalys for users and developers.

The applicability of the ESIS/Imalys indicators are demonstrated through three ecological applications, namely: (1) monitoring landscape diversity, (2) monitoring landscape structure and landscape fragmentation, and (3) monitoring land use intensity and its impact on ecosystem functions.

Further publications on the ESIS/Imalys tool with sample data and model calculations are planned, and both the data and derived indicators will be made openly available to users. The set of indicators will be continuously developed and expanded. The ESIS/Imalys tool is directly coupled with ecological models such as hydrological and agent-based models. Future plans include the integration of in situ measurements and punctual time series analysis to calibrate and validate the RS data used. The version currently available only on the Linux platform will be converted into a “container version” to make the tool platform-independent. RS indicators, which are quantified based on spectral raster traits could also be included in the semantic data integration. The ease of using ESIS/Imalys, optimised for a simple PC despite the large amount of RS data, makes it another important tool for research and application to monitor and derive ecosystem indicators from local to global scale.

**Author Contributions:** Conceptualization, A.L. and P.S.; methodology, A.L., P.S. and J.B.; software, P.S.; formal analysis, R.G.; investigation, P.S. and A.L.; resources, P.S., R.G. and J.B.; writing—original draft preparation, A.L. and P.S.; writing—review and editing, A.L., P.S., J.B., M.P., T.W., R.G. and E.B.; visualization, A.L., P.S. and T.W.; supervision, J.B.; project administration, J.B., P.S. and A.L.; funding acquisition, J.B. All authors have read and agreed to the published version of the manuscript.

**Funding:** This research received no external funding.

**Data Availability Statement:** The Imalys source code is open source (GPLv3), hosted and maintained in the Helmholtz Codebase: <https://doi.org/10.5281/zenodo.8116370>. There is also a complete documentation of all of the methods, functions and indicators derived, which can be found in the openly available Imalys manual.

**Acknowledgments:** Our special thanks go to the Helmholtz Centre for Environmental Research—UFZ and the TERENO project funded by the Helmholtz Association and the Federal Ministry of Education and Research for providing the remote sensing research. The authors gratefully acknowledge the German Helmholtz Association for supporting the activities of research data science approaches and advanced data technologies. We also thank the Helmholtz Association and the Federal Ministry of Education and Research (BMBF) for supporting the DataHub Initiative of the Research Field Earth and Environment. The DataHub enables an overarching and comprehensive research data management, following FAIR principles, for all Topics in the Program Changing Earth—Sustaining our Future.

**Conflicts of Interest:** The authors declare no conflicts of interest.

## Appendix A. Process Chain Example

```
IMALYS [import seasonal image]
home
  directory=/home/c7sepe2/.imalys
  clear=true
  log=/home/c7sepe2/METAMAP/c1114_Sy1t
import
  database=/media/c7sepe2/STOCK3/Landsat-89/2023/center.csv
  distance=1.00
  frame=/home/c7sepe2/METAMAP/v_TK-100/ c1114.gpkg
  quality=0.86
  period= 20230801-20231031
  bands=_B2, _B3, _B4, _B5, _B6, _B7
  factor=2.75e-5|
  offset=-0.2
  cover=0.9
  warp=32632
  pixel=30
compile
  search=LC0*.hdr
reduce
  select=compile
  execute=bestof
export
  select=bestof
  target=/home/c7sepe2/METAMAP/c1114_Sy1t_bestof_20230801-20231031.tif
```

### Appendix B

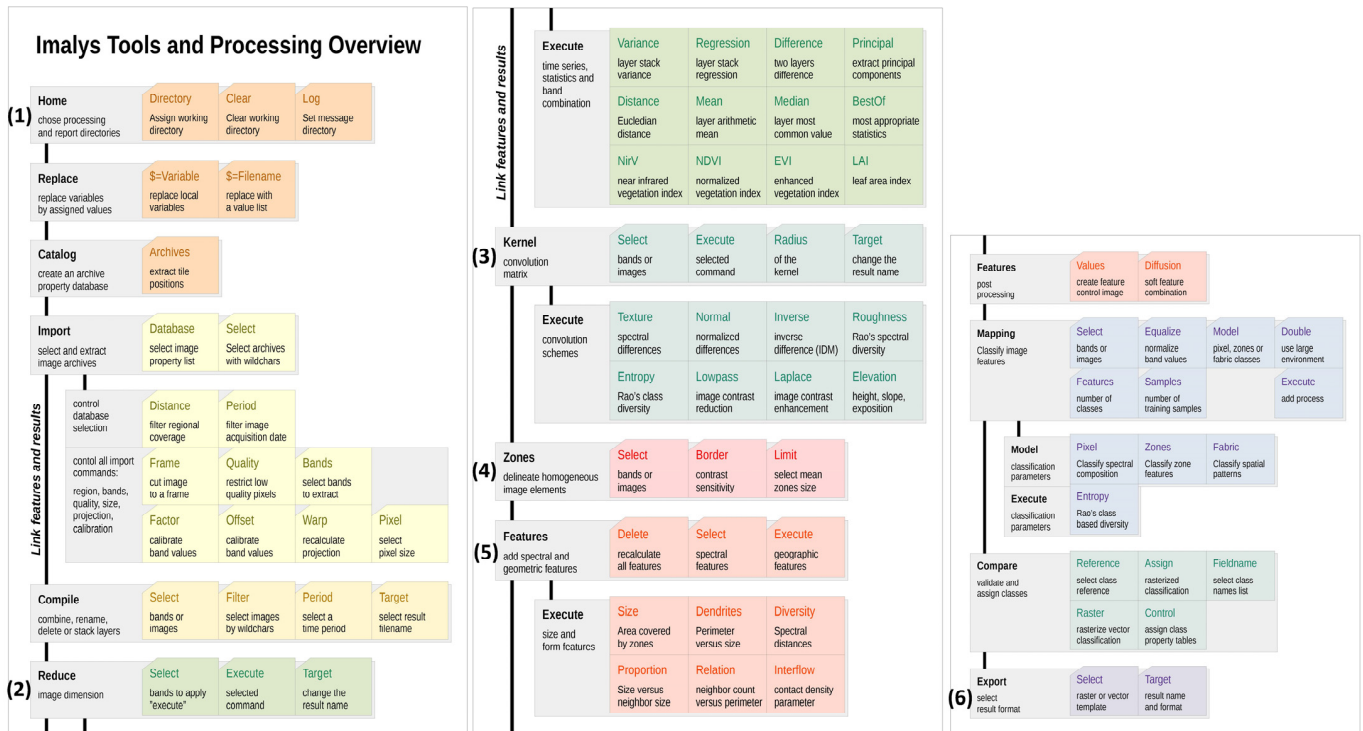


**Figure A1.** Flowchart of the ESIS Imalys library consisting of six blocks. Block 1–3 is the pixel area of Imalys: (1) data import, remote sensing data processing, remote sensing data management (functions—marked purple); (2) raster processes, statistical raster information, replaced image bands, time series analysis, statistics; (3) kernel processes for calculating and deriving raster-based indicators (functions—marked orange). Block 4–5 is the zones and pixel area of Imalys: (4) Segmentation of zones (polygons), formation of borders, derivation of raster- and zone-based indicators for each zone. All pixel results can be taken as mean values for each zone (functions—marked red). (5) Extraction of classes and objects by unsupervised classification, correlate features (functions—marked purple). (6) Export of results including format conversion as raster, vector or table (functions—marked green). The Imalys source code is open source (GPLv3), hosted and maintained in the Helmholtz Codebase: <https://doi.org/10.5281/zenodo.8116370>. There is also a complete documentation of all of the methods, functions and indicators derived, which can be found in the openly available Imalys manual.

**Table A1.** Functions, tools, descriptions and formulas. The following tables show tools and traits and their definitions by means of a text box and a formula. The trait names also serve as commands in the Imalys process chain, as a file name of the process results, and as field names in tables. Therefore, the names are short and can have a much wider meaning in general usage. Imalys tools are aids to execute the process chain.

Spectral		
Traits	Description	Formula
Variance	Variance based on standard deviation The “variance” command determines the variance of individual pixels based on a standard distribution for all of the bands in source. For multi-image stacks, “Variance” determines the variance for each band separately and gives the result as a multispectral image of the variances. The result can be further reduced to a one band image with the first principal component of all bands using “principal”.	$\frac{\sum_i v^2 - (\sum_i v)^2}{n-1} / n$ v: values i: items n: item count

Table A1. Cont.

Spectral		
Traits	Description	Formula
Regression	Regression based on standard deviation "Regression" returns the regression of individual pixels of all bands in source. "Regression" uses the temporal distance of the recordings from the metadata of the images. To do this, the images must have been imported with "extract" or have been dated afterwards with "extend". Similar to "variance", "regression" determines the regression for each band separately if multispectral images are provided and gives a multispectral regression.	$\frac{\sum_i t \cdot v - \sum_i t \sum_i v / n}{\sum_i v^2 - (\sum_i v)^2 / n}$ t: time v: values i: items n: item count
Difference	Euclidean distance of two n-dimensional properties "Difference" gives the difference between the values of two bands or two images. For multispectral images, "difference" generates a result for each band separately and returns a multispectral image of the differences for all bands.	$v_a - v_a$ v: pixel value
Vegetation	<i>Near-infrared vegetation index (NIRv)</i> The NIRv index is calculated as the product of near infrared radiation and the normalised difference of the red and the near-infrared radiation. The calculation follows the most common NDVI definition but shows better mapping in sparsely vegetated areas. Vegetation indices were introduced to estimate the plant-covered proportion of the landscape. The result depends on the photosynthetic activity of the plants. Vegetation indices try to quantify the photosynthetically active radiation (PAR) as a measure of plant metabolism. There are about 20 different approximations described [42].	$\frac{(N-R)}{(N+R)} \cdot N$ N: near-infrared value R: red band value Value range: 0..1
Principal	"Principal" gives the first principal component of all bands. The first principal component reflects the brightness or density of all image bands. Imalys uses this process as brightness in several other cases.	$\sqrt{\sum_i v_i^2}$ v: values i: items
Mean	Arithmetic mean, bands or images Mean gives the arithmetic mean of all image bands provided. For multispectral images, "mean" is individually calculated for each band. The process returns a multispectral image of mean values.	$\frac{\sum_i v_i}{n}$ v: values i: items n: item count
Median	<i>Most common value for each pixel from a stack of bands</i> "Median" reflects the most common value of each pixel in a stack of bands or images. For multiple image stacks, "median" is individually calculated for each band. Median will mask rare values. Image disturbances like clouds or smoke will be masked if more than half of all pixels show an unchanged value.	Value in the middle of a sorted value list.
Convolution		
Traits	Description	Formula
Texture		
Normal	<i>Normalised texture</i> "Normal" collects the first principal component of all normalised differences between two neighbouring pixels within a given kernel and returns the mean. Landscape diversity increases with texture. The normalised texture is independent of brightness or illumination (shadows). In contrast to Rao's "entropy" or "roughness", "normal" will return similar values for regular and randomly distributed patterns.	$\sqrt{\sum_b \left( \frac{v_i - v_j}{v_i + v_j} \right)^2}$ v <sub>i</sub> : pixel value v <sub>j</sub> : neighbour pixel value Value range: 0..1
Inverse	Inverse difference moment (IDM) "Inverse" creates a new image with the inverse difference moment (IDM) proposed by Haralik (Haralik 1979). "Inverse" is particularly high in dark regions and low in bright regions. It can complement "texture" and has proved useful in the analysis of settlement structures.	$\sqrt{\sum_b \frac{1}{(v_i - v_j)^2}}$ v: values l <sub>j</sub> : neighbor pixels b: bands

Table A1. Cont.

Convolution		
Traits	Description	Formula
Roughness (Rao's Q Index)	<p><i>Rao's diversity based on pixels</i></p> <p>As "Texture" does, Rao's approach evaluates the spectral difference of individual pixels, but does not only compare neighbouring pixels, but all pixels within the kernel. Unlike the classical "texture" or "normal" indicators, "roughness" is insensitive for the spatial distribution of the pixels within the kernel.</p> <p>"Roughness" returns a measure for landscape diversity based on pixel differences within a given kernel. Most like "Entropy", each distribution of a given set of pixels will produce the same result.</p>	$\sum_{ij} (d_{ij} \cdot p_i \cdot p_j)$ <p><math>d_{ij}</math>: Density difference between pixel (i) and (j)  <math>p_i, p_j</math>: Frequency of pixel values (I) and (j)            Value range not limited</p>
Entropy	<p><i>Rao's entropy (diversity) based on classes</i></p> <p>"Entropy" collects the number of class differences and class similarities for all pixel combinations within a given kernel. The number of different class combination is scaled with the spectral differences between the classes.</p> <p>Entropy needs a classification of the images to run. The easiest way to obtain this classification is to call the "Mapping" trait. Alternatively, "Entropy" can use an existing classification.</p> <p>"Entropy" returns the diversity of landscape classes within a given kernel. "Entropy" ignores small landscape differences that are represented by the same class and returns a more abstract level. Rao's approach is insensitive to the distribution of the pixels within the kernel. A chessboard-like distribution of two classes will produce the same result as two homogeneous areas with the same classes.</p>	$\sum_{kl} (d_{kl} \cdot p_k \cdot p_l)$ <p><math>d_{kl}</math>: spectral Distance between the the classes (k) and (l)  <math>p_k</math>: frequency of class (k)  <math>p_l</math>: frequency of class (l)            Value range not limited</p>
Lowpass	<p>Reduce local contrast</p> <p>"Lowpass" reduces the local contrast of the image data according to the selected "radius".</p> <p>The process reduces the local contrasts and can fix small bugs. "Lowpass" uses a kernel with a normalised Gaussian distribution. The kernel size can be selected freely. Imalys implements large kernels through an iterative process to significantly reduce the processing time.</p>	$\sum_{ij} (v_{ij} \cdot k_{ij})$ <p><math>v</math>: image values  <math>k</math>: kernel values  <math>l_j</math>: kernel index</p>
Laplace	<p>Enhance local contrast</p> <p>A "Laplace" transformation (Mexican head function) enhances the image contrast and can make lines and closed shapes clearly visible. Imalys implements the transformation as the difference between two Gaussian distributions with a different radius. The parameters "inner" and "outer" control the size (kernel radius) of the two distributions.</p>	$\sum_{ij} (v_{ij} \cdot (k_{ij} - g_{ij}))$ <p><math>v</math>: values  <math>k</math>: inner kernel  <math>g</math>: outer kernel  <math>l_j</math>: kernel indices</p>
Create Zones		
Traits	Description	Formula
Zones	<p>Delineated homogeneous image elements</p> <p>The "zones" process delineates a seamless network of zones that completely covers the image. The zones are assigned with the spectral signatures of the image data as attributes. The attributes can be expanded (below).</p> <p>"Zones" were introduced to provide a structural basis that can be used for landscape diversity and other structural features. Zones allow for easy transformation of raster images to a vector format like maps.</p>	<p>Structural delineation similar to an inverse watershed.</p>
Dendrites	<p><i>Quotient of zone perimeter and zonal size</i></p> <p>"Dendrites" returns the quotient between perimeter and size of single zones. Both values grow with larger zones, but the size grows faster. Large zones will show lower values than smaller ones with the same shape.</p> <p>"Dendrites" was introduced as a size-independent measure of spatial diversity. Long and small zones may be quite large but their role in landscape diversity is similar to that of small zones. Small, thin or dendritically shaped zones show high values, large compact zones show the lowest.</p>	$V_r = \frac{p_z}{s_z}$ <p><math>v_r</math>: result value  <math>p_z</math>: perimeter (zone)  <math>s_z</math>: size (zone)            Value range: 0 . . 4</p>

Table A1. Cont.

Create Zones		
Traits	Description	Formula
Diversity	<p>Spectral diversity for all neighbour zones</p> <p>“Diversity” is calculated as the mean principal component of all spectral differences between all pixels of a single zone. This includes all pixel borders to neighbour zones and also all pixel borders within the zone. The differences are calculated with the zonal mean values, not with individual pixels.</p> <p>“Diversity” was introduced as size-dependent spectral diversity. The principal component intensifies the contrast of single bands. High values indicate small zones and high spectral differences. Small or narrow zones embedded in large zones are emphasized.</p>	$\frac{\sqrt{\sum_{i,n}(v_i-v_n)^2}}{b_p}$ <p><math>v_i</math>: zonal value  <math>v_n</math>: neighbour value  <math>b_p</math>: pixel borders  Value range: 0..1 for reflection values</p>
Proportion	<p>Size difference between central zone and all neighbours</p> <p>“Proportion” returns the relation between the size of a single zone and all its neighbours. The result is calculated as difference between the size of the central zone and the mean size of its neighbours. As the size is given on a logarithmic scale, the “mean” is not an arithmetic but a geometric mean. The result will be negative if the central zone is smaller than its neighbours.</p> <p>“Proportion” resembles a texture for zonal sizes. Proportion is independent of the individual size of a zone. Values around zero indicate equally sized neighbour zones. Zones with smaller neighbours show positive values; zones with larger neighbours are negative.</p>	$\frac{\sum_j \ln(s_i) - \ln(s_j)}{n}$ <p><math>s_i</math>: size, central zone  <math>s_j</math>: size, neighbour zone  n: number of neighbours</p>
Relation	<p>Quotient of cell perimeter and number of neighbours</p> <p>“Relation” is calculated as the relation between the perimeter of the zone and the number of neighbouring zones.</p> <p>“Relation” was introduced as an indicator for spatial diversity. Large zones and small zones with few neighbours will have large values. Small zones with many neighbours will show higher values. Like “Dendrites”, “relation” also returns information about the shape and the connection of the zones. Zones with many connections may provide paths for animal travels and enhance diversity.</p>	$R = \frac{p}{c}$ <p>R: relation  p: perimeter  c: number of neighbours</p>
Size	<p>Size of one zone given as natural logarithm</p> <p>The zonal size is calculated from the sum of pixels covering the zone.</p> <p>Landscape diversity increases with smaller zones</p>	$S = \ln(a)$ <p>a: area of zone [ha]</p>
Diffusion	<p>Smooth properties in a zones network</p> <p>The algorithm for value equalisation in zones mimics diffusion through membranes (borders). In the process, features “migrate” into the neighbouring zone like soluble substances and combine with existing concentrations. The intensity of diffusion depends on the length of the common border and the number of iterations. The size of the zones does not matter.</p> <p>The process is only controlled by the number of iterations. Each iteration includes a new layer of contributing zones. The influence of distant zones on the central zone decreases with distance. Entries over 10 are still allowed, but rarely have a visible effect.</p>	$\sum_t (a \cdot s) + \sum_{ij} (a_j \cdot b - a_i \cdot b)$ <p>a: attribute  s: zone size  b: border length  ij: zone indices  t: iterations (time)</p>
External		
Values	<p>Raster representation of a vector map with attributes</p> <p>“Values” creates a multiband raster image from vector borders and the attributes of the different polygons. “Values” mainly serves as a control feature.</p>	Raster image from vector polygons
Classification		
Trait/Tool	Description	Process
Pixel	<p>“Pixel” classifies spectral combinations</p> <p>“Pixel” selects a pixel-oriented classification of the image data. The process uses all bands of the provided image. The process is controlled only by the number of classes in the result. All values should have a comparable value range, as calibrated images do.</p>	Fully self-adjusting classification of all pixel values

Table A1. Cont.

Classification		
Trait/Tool	Description	Process
Features	“Features” classifies spectral and spatial properties of zones “Features” selects the classification of zones based on their features. The process is controlled by the selected features and by the number of classes in the result. Each feature can be selected individually. As with “pixels”, the value range of the features should be comparable.	Fully self-adjusting classification of all zones’ features
Fabric (Objects)	“Fabric” creates and classifies image objects In this context, adjacent zones with an individual combination of different features are called objects. Object types (classes) and image objects are created during the same process. The object definition relays only on the borders between different types of zones. Thus, objects are characterized by their spatial pattern.	Fully self-adjusting delineation and classification of image objects based on zones with different features.
Compare	Compare a mapping with a reference Automated classification is driven by image features. Real classes are not necessarily defined by their appearance. “compare” allows for evaluating if and up to what degree real classes can be detected by image features.	Confusion matrix for false and true detection and denotation
Rank	Correlate distributions “Rank” calculates a correlation coefficient based on a rank correlation model after Spearman. A rank correlation is independent of the basic value distribution. Therefore, it can be used for each set of data.	$1 - 6 \frac{\sum_i (r_i - s_i)^2}{n \cdot (n^2 - 1)}$ r,s: item rank i: item index n: item count
Export		
Traits	Description	Process
Raster	Export values using an image raster format Images and processing results can be exported in 48 different raster formats (according to most recent gdal library). Raster export includes vector-based process results. Standard format is ENVI labelled.	gdal library
Vector	Export values using a vector format Vector-based results can be exported using 23 different vector formats (according to most recent gdal library). Vector export includes automated transformation for most of the raster data. Standard formats are ESRI Shape and CSV.	gdal library
Table	Export tables using a table format Value grids can be exported in different database and spreadsheet formats. Table export includes tables linked to raster or vector data. The standard format is CSV.	gdal library

## References

- Intergovernmental Panel on Climate Change. *Climate Change and Land*; Cambridge University Press: Cambridge, UK, 2022; ISBN 9781009157988.
- Skidmore, A.K.; Coops, N.C.; Neinavaz, E.; Ali, A.; Schaepman, M.E.; Paganini, M.; Kissling, W.D.; Vihervaara, P.; Darvishzadeh, R.; Feilhauer, H.; et al. Priority list of biodiversity metrics to observe from space. *Nat. Ecol. Evol.* **2021**, *5*, 896–906. [[CrossRef](#)] [[PubMed](#)]
- Lausch, A.; Selsam, P.; Pause, M.; Bumberger, J. Monitoring vegetation- and geodiversity with remote sensing and traits. *Philos. Trans. R. Soc. A Math. Phys. Eng. Sci.* **2024**, *382*, 20230058. [[CrossRef](#)] [[PubMed](#)]
- Lausch, A.; Schaepman, M.E.; Skidmore, A.K.; Catana, E.; Bannehr, L.; Bastian, O.; Borg, E.; Bumberger, J.; Dietrich, P.; Glässer, C.; et al. Remote Sensing of Geomorphodiversity Linked to Biodiversity—Part III: Traits, Processes and Remote Sensing Characteristics. *Remote Sens.* **2022**, *14*, 2279. [[CrossRef](#)]
- Schrodt, F.; Vernham, G.; Bailey, J.; Field, R.; Gordon, J.E.; Gray, M.; Hjort, J.; Hoorn, C.; Hunter, M.L., Jr.; Larwood, J.; et al. The status and future of essential geodiversity variables. *Philos. Trans. R. Soc. A Math. Phys. Eng. Sci.* **2024**, *382*, 20230052. [[CrossRef](#)] [[PubMed](#)]
- Kuemmerle, T.; Erb, K.; Meyfroidt, P.; Müller, D.; Verburg, P.H.; Estel, S.; Haberl, H.; Hostert, P.; Jepsen, M.R.; Kastner, T.; et al. Challenges and opportunities in mapping land use intensity globally. *Curr. Opin. Environ. Sustain.* **2013**, *5*, 484–493. [[CrossRef](#)] [[PubMed](#)]
- Burkhard, B.; Kroll, F.; Nedkov, S.; Müller, F. Mapping ecosystem service supply, demand and budgets. *Ecol. Indic.* **2012**, *21*, 17–29. [[CrossRef](#)]



8. Haase, P.; Tonkin, J.D.; Stoll, S.; Burkhard, B.; Frenzel, M.; Geijzendorffer, I.R.; Häuser, C.; Klotz, S.; Kühn, I.; McDowell, W.H.; et al. The next generation of site-based long-term ecological monitoring: Linking essential biodiversity variables and ecosystem integrity. *Sci. Total Environ.* **2018**, *613–614*, 1376–1384. [[CrossRef](#)]
9. Mollenhauer, H.; Kasner, M.; Haase, P.; Peterseil, J.; Wohner, C.; Frenzel, M.; Mirtl, M.; Schima, R.; Bumberger, J.; Zacharias, S. Science of the Total Environment Long-term environmental monitoring infrastructures in Europe: Observations, measurements, scales, and socio-ecological representativeness Group on Earth Observations Global Earth Observation System of Systems. *Sci. Total Environ.* **2018**, *624*, 968–978. [[CrossRef](#)]
10. Weber, U.; Attinger, S.; Baschek, B.; Boike, J.; Borchardt, D.; Brix, H.; Brüggemann, N.; Bussmann, I.; Dietrich, P.; Fischer, P.; et al. MOSES: A Novel Observation System to Monitor Dynamic Events across Earth Compartments. *Bull. Am. Meteorol. Soc.* **2022**, *103*, E339–E348. [[CrossRef](#)]
11. Zhao, Z.; Martin, P.; Grosso, P.; Los, W.; de Laat, C.; Jeffrey, K.; Hardisty, A.; Vermeulen, A.; Castelli, D.; Legre, Y.; et al. Reference Model Guided System Design and Implementation for Interoperable Environmental Research Infrastructures. In Proceedings of the 2015 IEEE 11th International Conference on e-Science, Munich, Germany, 31 August–4 September 2015; pp. 551–556.
12. Likens, G.E. Aldo Leopold’s “Odyssey” and the development of the ecosystem concept and approach. *Socio-Ecol. Pract. Res.* **2022**, *4*, 17–18. [[CrossRef](#)]
13. Rocchini, D.; Santos, M.J.; Ustin, S.L.; Féret, J.; Asner, G.P.; Beierkuhnlein, C.; Dalponte, M.; Feilhauer, H.; Foody, G.M.; Geller, G.N.; et al. The Spectral Species Concept in Living Color. *J. Geophys. Res. Biogeosci.* **2022**, *127*, e2022JG007026. [[CrossRef](#)]
14. Cavender-Bares, J.; Gamon, J.A.; Townsend, P.A. *Remote Sensing of Plant Biodiversity*; Cavender-Bares, J., Gamon, J.A., Townsend, P.A., Eds.; Springer International Publishing: Cham, Switzerland, 2020; ISBN 978-3-030-33156-6.
15. Zarnetske, P.; Read, Q.; Record, S.; Gaddis, K.; Pau, S.; Hobi, M.; Malone, S.; Costanza, J.; Dahlin, K.; Latimer, A.; et al. Towards connecting biodiversity and geodiversity across scales with satellite remote sensing. *Glob. Ecol. Biogeogr.* **2019**, *28*, 548–556. [[CrossRef](#)]
16. Lausch, A.; Schaepman, M.E.; Skidmore, A.K.; Truckenbrodt, S.C.; Hacker, J.M.; Baade, J.; Bannehr, L.; Borg, E.; Bumberger, J.; Dietrich, P.; et al. Linking the Remote Sensing of Geodiversity and Traits Relevant to Biodiversity—Part II: Geomorphology, Terrain and Surfaces. *Remote Sens.* **2020**, *12*, 3690. [[CrossRef](#)]
17. Kussul, N.; Lavreniuk, M.; Skakun, S.; Shelestov, A. Deep Learning Classification of Land Cover and Crop Types Using Remote Sensing Data. *IEEE Geosci. Remote Sens. Lett.* **2017**, *14*, 778–782. [[CrossRef](#)]
18. Wellmann, T.; Haase, D.; Knapp, S.; Salbach, C.; Selsam, P.; Lausch, A. Urban land use intensity assessment: The potential of spatio-temporal spectral traits with remote sensing. *Ecol. Indic.* **2018**, *85*, 190–203. [[CrossRef](#)]
19. Xie, C.; Wang, J.; Haase, D.; Wellmann, T.; Lausch, A. Measuring spatio-temporal heterogeneity and interior characteristics of green spaces in urban neighborhoods: A new approach using gray level co-occurrence matrix. *Sci. Total Environ.* **2023**, *855*, 158608. [[CrossRef](#)]
20. Chabrilat, S.; Segl, K.; Foerster, S.; Brell, M.; Guanter, L.; Schickling, A.; Storch, T.; Honold, H.-P.; Fischer, S. EnMAP Pre-Launch and Start Phase: Mission Update. In Proceedings of the IGARSS 2022–2022 IEEE International Geoscience and Remote Sensing Symposium, Kuala Lumpur, Malaysia, 17–22 July 2022; pp. 5000–5003.
21. Cerra, D.; Marshall, D.; Heiden, U.; Alonso, K.; Bachmann, M.; Burch, K.; Carmona, E.; Dietrich, D.; Lester, H.; Knodt, U.; et al. The Spaceborne Imaging Spectrometer Desis: Data Access, Outreach Activities, and Scientific Applications. In Proceedings of the IGARSS 2022–2022 IEEE International Geoscience and Remote Sensing Symposium, Kuala Lumpur, Malaysia, 17–22 July 2022; pp. 5395–5398.
22. Coyle, D.B.; Stysley, P.R.; Chirag, F.L.; Frese, E.A.; Poullos, D. The Global Ecosystem Dynamics Investigation (GEDI) LiDAR laser transmitter. In *Infrared Remote Sensing and Instrumentation XXVII: 12–14 August 2019, San Diego, California, United States*; Strojnik, M., Arnold, G.E., Eds.; SPIE: Bellingham, WA, USA, 2019; p. 20.
23. Cawse-Nicholson, K.; Townsend, P.A.; Schimel, D.; Assiri, A.M.; Blake, P.L.; Buongiorno, M.F.; Campbell, P.; Carmon, N.; Casey, K.A.; Correa-Pabón, R.E.; et al. NASA’s surface biology and geology designated observable: A perspective on surface imaging algorithms. *Remote Sens. Environ.* **2021**, *257*, 112349. [[CrossRef](#)]
24. Le Provost, G.; Thiele, J.; Westphal, C.; Penone, C.; Allan, E.; Neyret, M.; van der Plas, F.; Ayasse, M.; Bardgett, R.D.; Birkhofer, K.; et al. Contrasting responses of above- and belowground diversity to multiple components of land-use intensity. *Nat. Commun.* **2021**, *12*, 3918. [[CrossRef](#)]
25. Palmer, M.W.; Earls, P.G.; Hoagland, B.W.; White, P.S.; Wohlgemuth, T. Quantitative tools for perfecting species lists. *Environmetrics* **2002**, *13*, 121–137. [[CrossRef](#)]
26. Rocchini, D.; Chiarucci, A.; Loiselle, S.A. Testing the spectral variation hypothesis by using satellite multispectral images. *Acta Oecol.* **2004**, *26*, 117–120. [[CrossRef](#)]
27. Conti, L.; Malavasi, M.; Galland, T.; Komárek, J.; Lagner, O.; Carmona, C.P.; Bello, F.; Rocchini, D.; Šímová, P. The relationship between species and spectral diversity in grassland communities is mediated by their vertical complexity. *Appl. Veg. Sci.* **2021**, *24*, e12600. [[CrossRef](#)]
28. Ustin, S.L.; Gamon, J.A. Remote sensing of plant functional types. *New Phytol.* **2010**, *186*, 795–816. [[CrossRef](#)]
29. Díaz, S.; Kattge, J.; Cornelissen, J.H.C.; Wright, I.J.; Lavorel, S.; Dray, S.; Reu, B.; Kleyer, M.; Wirth, C.; Colin Prentice, I.; et al. The global spectrum of plant form and function. *Nature* **2016**, *529*, 167–171. [[CrossRef](#)]

30. Lausch, A.; Erasmi, S.; King, D.; Magdon, P.; Heurich, M. Understanding Forest Health with Remote Sensing-Part I—A Review of Spectral Traits, Processes and Remote-Sensing Characteristics. *Remote Sens.* **2016**, *8*, 1029. [[CrossRef](#)]
31. Andersson, E.; Haase, D.; Anderson, P.; Cortinovis, C.; Goodness, J.; Kendal, D.; Lausch, A.; McPhearson, T.; Sikorska, D.; Wellmann, T. What are the traits of a social-ecological system: Towards a framework in support of urban sustainability. *NPJ Urban Sustain.* **2021**, *1*, 14. [[CrossRef](#)]
32. Lausch, A.; Blaschke, T.; Haase, D.; Herzog, F.; Syrbe, R.-U.; Tischendorf, L.; Walz, U. Understanding and quantifying landscape structure—A review on relevant process characteristics, data models and landscape metrics. *Ecol. Modell.* **2015**, *295*, 31–41. [[CrossRef](#)]
33. McGarigal, K.; Marks, B.J. *FRAGSTATS: Spatial Pattern Analysis Program for Quantifying Landscape Structure*; U.S. Department of Agriculture, Forest Service, Pacific Northwest Research Station: Portland, OR, USA, 1995.
34. McGarigal, K.; Cushman, S.A. The gradient concept of landscape structure. In *Issues and Perspectives in Landscape Ecology*; Cambridge University Press: Cambridge, UK, 2005; pp. 112–119.
35. Blaschke, T. Object based image analysis for remote sensing. *ISPRS J. Photogramm. Remote Sens.* **2010**, *65*, 2–16. [[CrossRef](#)]
36. Blaschke, T.; Hay, G.J.; Kelly, M.; Lang, S.; Hofmann, P.; Addink, E.; Queiroz Feitosa, R.; van der Meer, F.; van der Werff, H.; van Coillie, F.; et al. Geographic Object-Based Image Analysis—Towards a new paradigm. *ISPRS J. Photogramm. Remote Sens.* **2014**, *87*, 180–191. [[CrossRef](#)] [[PubMed](#)]
37. Kralisch, S.; Böhm, B.; Böhm, C.; Busch, C.; Fink, M.; Fischer, C.; Schwartze, C.; Selsam, P.; Zander, F.; Flügel, W.A. ILMS—A Software Platform for Integrated Environmental Management. International Congress on Environmental Modelling and Software. 206. Available online: <https://scholarsarchive.byu.edu/iemssconference/2012/Stream-B/206> (accessed on 19 March 2024).
38. Zander, F.; Kralisch, S.; Busch, C.; Flügel, W.-A. Data management in multidisciplinary research projects with the River Basin information System. *EnvironInfo* **2012**, 143–149.
39. Selsam, P.; Schwartze, C. Remote Sensing Image Analysis Without Expert Knowledge—A Web-Based Classification Tool On Top of Taverna Workflow Management System. *IOP Conf. Ser. Earth Environ. Sci.* **2016**, *44*, 042020. [[CrossRef](#)]
40. Selsam, P.; Gey, R.; Lausch, A.; Bumberger, J. Imalys—Image Analysis (0.1). *Zenodo* **2023**. [[CrossRef](#)]
41. Rocchini, D.; Bacaro, G.; Chirici, G.; Da Re, D.; Feilhauer, H.; Foody, G.M.; Galluzzi, M.; Garzon-Lopez, C.X.; Gillespie, T.W.; He, K.S.; et al. Remotely sensed spatial heterogeneity as an exploratory tool for taxonomic and functional diversity study. *Ecol. Indic.* **2018**, *85*, 983–990. [[CrossRef](#)]
42. Badgley, G.; Field, C.B.; Berry, J.A. Canopy near-infrared reflectance and terrestrial photosynthesis. *Sci. Adv.* **2017**, *3*, e1602244. [[CrossRef](#)]
43. Rocchini, D.; Marcantonio, M.; Ricotta, C. Measuring Rao’s Q diversity index from remote sensing: An open source solution. *Ecol. Indic.* **2017**, *72*, 234–238. [[CrossRef](#)]
44. Rocchini, D.; Luque, S.; Pettorelli, N.; Bastin, L.; Doktor, D.; Faedi, N.; Feilhauer, H.; Féret, J.; Foody, G.M.; Gavish, Y.; et al. Measuring  $\beta$ -diversity by remote sensing: A challenge for biodiversity monitoring. *Methods Ecol. Evol.* **2018**, *9*, 1787–1798. [[CrossRef](#)]
45. Xu, Q.; Wang, P.; Shu, W.; Ding, M.; Zhang, H. Influence of landscape structures on river water quality at multiple spatial scales: A case study of the Yuan river watershed, China. *Ecol. Indic.* **2021**, *121*, 107226. [[CrossRef](#)]
46. Pu, X.; Cheng, Q. Unraveling the impacts of multiscale landscape patterns and socioeconomic development on water quality: A case study of the National Sustainable Development Agenda Innovation Demonstration Zone in Lincang City, Southwest China. *J. Hydrol. Reg. Stud.* **2024**, *51*, 101660. [[CrossRef](#)]
47. Xiao, H.; Su, R.; Luo, Y.; Jiang, Y.; Wang, Y.; Hu, R.; Lin, S. Effects of land cover patterns on pond water nitrogen and phosphorus concentrations in a small agricultural watershed in Central China. *Catena* **2024**, *237*, 107800. [[CrossRef](#)]

**Disclaimer/Publisher’s Note:** The statements, opinions and data contained in all publications are solely those of the individual author(s) and contributor(s) and not of MDPI and/or the editor(s). MDPI and/or the editor(s) disclaim responsibility for any injury to people or property resulting from any ideas, methods, instructions or products referred to in the content.